PROCEEDINGS, Twenty-Eighth Workshop on Geothermal Reservoir Engineering
Stanford University, Stanford, California, January 27-29, 2003
SGP-TR-173

FRACTURE RESERVOIR CHARACTERIZATION BY FIBER-OPTIC DISTRIBUTED TEMPERATURE LOG

Naotsugu IKEDA

Shincoh Co.
1-3-13 Higashiminato, Kokurakita-Ku,
Kitakyushu, Fukuoka, Japan 803-0802
e-mail:ikeda_naotsugu@shincoh.co.jp

ABSTRACT

One of the important features of the fiber-optic distributed temperature log is its ability to acquire continuous, instantaneous and simultaneous temperature profile along the entire wellbore. Series of successive temperature profiles sampled every one minute or so enable to analyze transient temperature phenomena, which may pertain to important reservoir properties. For example, when change of rate occurred to the fluid flow such as due to water injection, the temperature profile over the section exhibits transient phenomena associated with the fluid flow. The characteristics of the phenomena depend on several factors including the flow profile which itself exhibits transient nature depending on fluid compressibility, permeability and reservoir extent, the original temperature profile, the temperature of injected fluid and that of the reservoir fluid flowing into the wellbore, the degree of rate alteration, well geometry, flow regime and etc.

This transient state eventually converges to pseudo-steady state and so does the temperature profile. But especially during the early time of its progress, the movement of fluid mass can be deduced by the movement of the temperature profile which has specific characteristics pertaining to the fluid mass. Especially when the adjacent wellbore fluid masses exhibit large temperature contrast such as for cold injected water and hot thermal brine, the fluid flow in wellbore is clearly seen by the movement of the corresponding temperature boundary.

In other words the sequential temperature profiles measured by fiber-optic distributed temperature log could render fluid flow profile along the wellbore. Because the temperature profile along the entire wellbore is simultaneously acquired, the derived flow profile has no time delay over different depths. Effect of flow mixtures from fractures at several different depths can be clearly identified not only by the flow speed but also by the shift on temperature profile. Since the measurement principle for the fluid flow detection employed by the fiber-optic distributed temperature log and by the spinner is very different, these two methods can complement each other to improve interpretation quality which is not so obvious all the time.

The application of the fiber-optic distributed temperature log is particularly interesting for geothermal wells where fresh water flows in and out of the permeable beds, as one can additionally deduce pressure profile from the temperature profile and can clearly differentiate characteristics of several fractures which belong to different hydrological regimes. The fiber-optic distributed temperature log if coupled with appropriately designed measurement procedure, may render enough information to characterize each layer of permeable beds. In this paper, one of such studies for a geothermal producer located in the northern Kyushu, Japan is presented. The outcome is interesting as it clearly demonstrates presence of annulus flow behind casing, presence of pressure difference in the different layers or a derivation of coherent reservoir permeability and more.

MEASUREMENT SYSTEM

The detail explanation of the measurement system is not repeated as it elsewhere appeared as in Ikeda et al.(2000) or in Ikeda(2002). The two major components of the measurement system are the surface instrument (SUT-110, Sumitomo Electric Industries) which emits laser pulse as well as receives scattered light to be processed to derive temperature output. The other is downhole fiber optic sensor, which is made of a single ended fiber (50/125 GI with polyamide and silicone resin coating), housed in coaxial metal double tubes. Hydrogen causes malignant effect on the transmission characteristics of the optical fiber especially at elevated temperature. Number of studies as to the mechanism involved in this process have been filed and it is widely accepted that the rate of hydroxyl formation and the hydrogen partial pressure has clear relationship, e.g. as in Iino et al.(1990) and Stone(1987). The double tubes

mechanism employed in the system is designed to allow nitrogen flushing in order to reduce partial pressure of hydrogen, thus suppressing the adverse effect on the measurement caused by the hydrogen absorption.

The nitrogen flushing was tested effective under 170 degrees Celsius for three months(Sumitomo Electric Industries (1995)). The current sensors neither indicate measurement degradation after several runs and hours of use including 286 degrees Celsius for the one sensor and for the other one going through 43 hours of continuous survey under 275 degrees Celsius. Horner plot from one of the above continuous surveys is shown in Fig.1 for three depths. All show smooth and monotonic transition, supporting the measurement validity during the survey period. Furthermore, prior to and after the survey, Stokes and Anti-Stokes intensities vs. cable distance ware measured with the cable at surface as in Fig.2. The temperature was nearly uniform throughout the cable and the ambient temperature at the time of the two measurements was similar, which is evidenced by the fact that the Anti-Stoke, which is more sensitive to temperature, show little separation. Those curves do not indicate any sign of change on the cable characteristics, which further proves the optical fiber suffered little from hydrogen intrusion.

Normann et al.(2000) and Smithpeter et al.(1999) reported that the measurement degradation due to hydrogen diffusion into the fiber started immediately after the installation in the wellbore. The wavelength of the laser light used in our system is shorter than the one used for their experiment, hence hydrogen effect on ours is expected to be less. In addition, the other detail fiber specification as well as those for the surface instruments may differ between ours and theirs. Nonetheless our fiber would neither be able to avoid hydrogen effects, even though at different magnitude, if there is no nitrogen flushing. From the fact it was prevented for almost two days under such elevated temperature, we expect that the system would be able to withstand at last for a few weeks under upto 300 degrees Celsius.

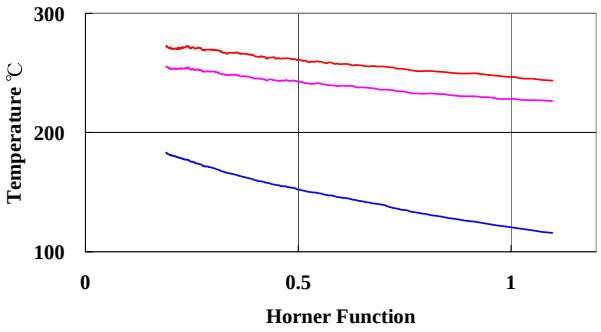

Figure 1. Horner plot for a few selected depths. s.t.=6~48 hours at 67 sec. sampling interval.

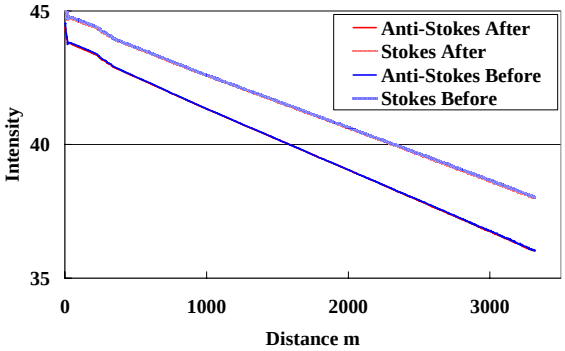

Figure 2. *Plot of Stokes and Anti-Stokes Intensity vs. Cable distance measured on Dec.19 and on Dec.22,2002.*

INTERPRETATION METHODOLOGY

The interpretation method normally used for the conventional temperature log assumes temperature profile in wellbore is under equilibrium or similar state as point sensor needs some time to complete survey over the required interval. Consequently it is impossible to analyze rapidly changing temperature profile, thus what behind causing such phenomena. It has been accepted as norm since otherwise there have been no alternatives.

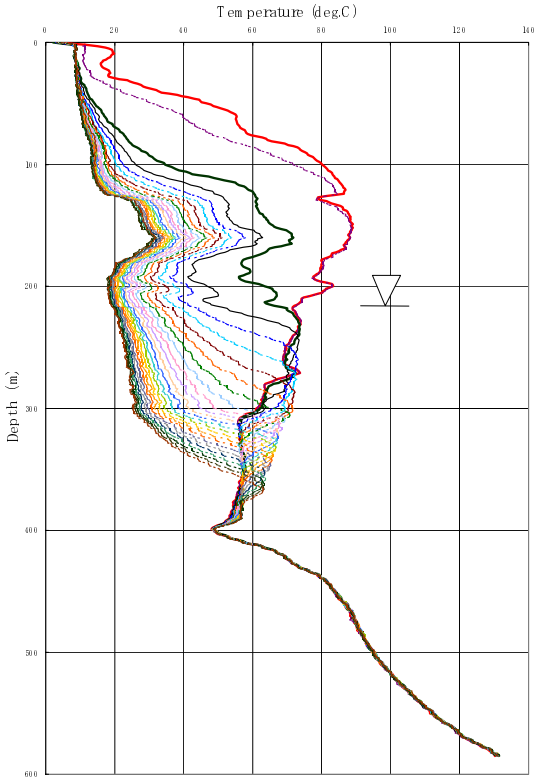

Figure 3. Successive temperature profiles during water injection to a re-injection well recorded by the fiber optic temperature log.

The fiber-optic distributed temperature log revolutionized the way of temperature acquisition and created a new interpretation methodology. Ikeda et al (2000) and Ikeda (2002) described a way to derive fluid flow profile from successive temperature profiles while injecting water or after stopping the injection. Fig.3 shows an example taken during injecting water, which clearly indicates the flow slowed down at 300m. This way of deriving flow profile from the temperature profiles leads to further application in reservoir evaluation.

In the past it has been tried to estimate fluid column pressure profile from the static temperature profile assuming wellbore fluid is fresh. Given z is vertical depth from the water level, the water head is expressed as follows;

$$P(z) = P_{water\_level} + \int_{water\_level}^{z} \rho(z)dz$$

where $P(z)$: fluid pressure , P_{water_level} : pressure at water level, $\rho(z)$:water density under the condition of the depth z.. To estimate this parameter under transient state had not been possible until the fiber-optic distributed temperature log became available. Ikeda (2002) tested the accuracy of this derivation both under static condition and under flowing condition and they seemed to be reasonably matched with those of quartz memory gauge.

Once the flowrate under given fluid pressure is known, it is not hard to derive intrinsic fluid pressure and injectivity index for the specific permeable bed. In addition, the intrinsic fluid temperature is better estimated with the fiber-optic distributed temperature log since the change of the fluid temperature is accurately assessed when the flowrate of the formation fluid flowing into the wellbore has changed due to such actions as injecting water or stopping it. The papers above described a way to characterize each permeable bed by the parameters such as intrinsic formation fluid pressure, temperature and injectivity index. They could be useful when making well-to-well correlation for each permeable bed.

Much of the studies are still under the way. But one of the preliminary results is to analyze structure of the open fracture in reservoir. *Fig.4-1* through to *Fig.4-4* are 3-D views of the well trajectories for wells in re-injection area, while rotating 30 degrees between the each figure. High permeable beds are marked with attributes characterizing their specific features. At one azimuth angle, many of the marks are more or less lined up on a straight line, which may correspond to the possible fault. The clusters along the line contain those marks with very different feature. It may be suggesting that the major structure consists of several high permeable planes, which however have rather low hydraulic conductivity between them. Thus it may be important to assess not only the overall structure but also the detail one to understand the fracture type reservoir.

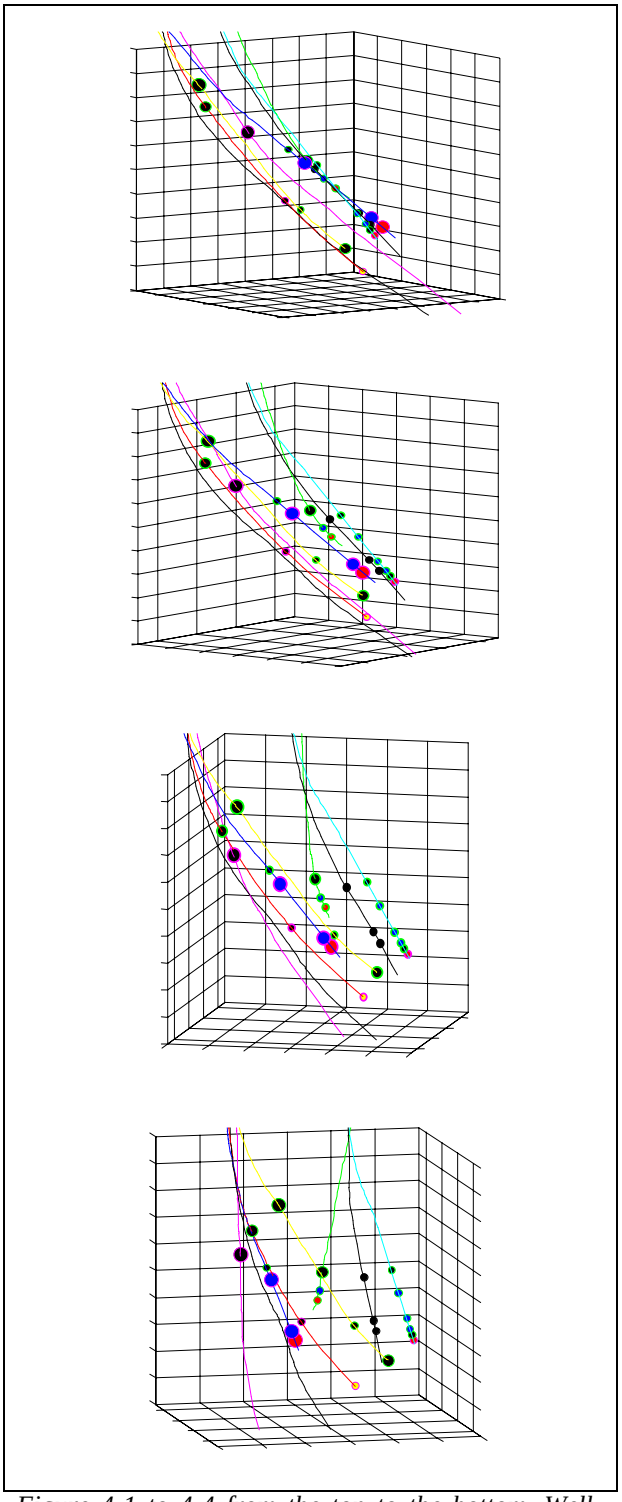

Figure 4-1 to 4-4 from the top to the bottom. Well trajectories of selected re-injection wells with analyzed permeable zones while rotating anti-clockwise at 30 degrees each step.

ANNULUS FLOW BEHIND CASING

A production well was completed with 7” liner, which was in part cemented in order to plug off permeable zone which showed excessive hydraulic connectivity to the nearby wells. In order to check if there is any leakage from the liner hanger, the fiber-optic distributed temperature log was deployed.

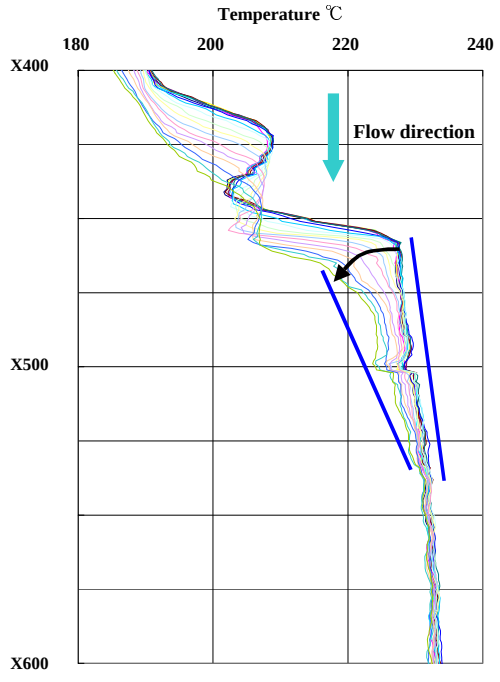

Figure 5. Temperature profiles recorder during water injection. Time sampling interval between each profile is about 67 seconds.

Since the distance between the lost circulation zones in the cemented section and the expected reservoir was a few hundred meters apart, we expected that these would belong to different hydrological regimes, which consequently would render cross-flow between them. If some amount of water is injected to alter the existing cross-flow and the temperature profile, it may be possible to see state of the flow during water injection as well as one for static condition.

The temperature profiles before and during the water injection is shown in Fig.5. The static temperature profiles as seen before the water injection is rather flat in the 7” liner which is indicative of the presence of cross flow. When water is injected, the wellbore fluid started moving downward, as you may see it from the gradual shift on the temperature peak, originally at about x425m. If there is no leakage, gradual descending of the fluid which is cooler by 25~30 degrees Celsius, into 7” liner would have been evident on the temperature profiles. However once the cool water front immediately reached about x550 m, it did not seem to advance any further. In stead the temperature profile above that depth looked like opening fan with x1550m as its pivotal point. One explanation to this is that the cold fluid mostly flows through the annulus behind 7” liner and finally escapes out to formation at around x550m. Transition of temperature profiles after stopping injection as shown in Fig. 6 seems to indicate presence of upward cross flow under the static condition. Based on the above injection and post-injection temperature profiles, the flow condition of the well was diagnosed as shown in *Fig. 7*.

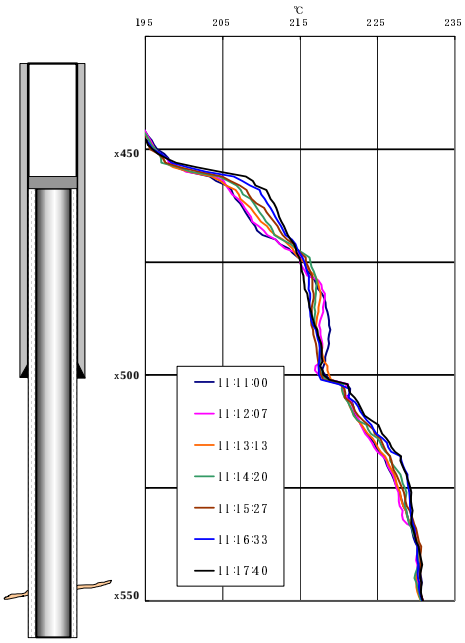

Figure 6. Temperature profiles just after stopping water injection.

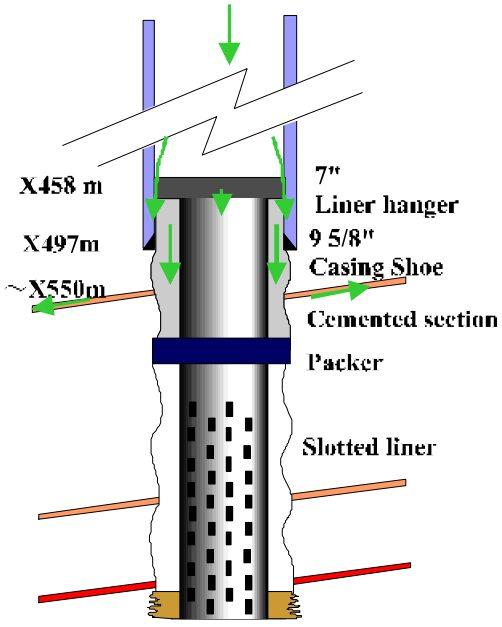

Figure 7. Well configuration below 7” liner hanger and diagnosed well condition. .

TRANSIENT WELL TEST AND VARIABLE RATE CONVOLUTION

After the leak assessment was done for the above production well, much higher rate(~800 liter/min.) of water was injected for longer period(~35minutes) while the temperature profiles were recorded by the fiber-optic distributed temperature log. We continued recording the temperature profiles after stopping water injection for about one hour. This relatively large rate of injection created enough water head to cause downhole flow till the bottom most permeable bed which was located near TD.

The temperature profiles at around the water level is shown in Fig. 8 during water injection and in Fig. 9 after stopping injection. For both events the transition of the water level is very clear. Therefore it is possible to deduce water head at any given depth during the testing period. In addition, as described earlier, the downhole flowrate can be computed by the temperature profiles. With downhole flowrate and pressure available, it may be treated as a kind of variable-rate well testing. Derivation of well permeability by rate-variable convolution technique while making simultaneous downhole pressure and flow measurement has been well established, e.g. Stewart(1983) and Simmon(1986).

The pressure response of a variable rate system can be expressed by the following equation as shown in NEDO(1993);

$$P_w = P_i + m\left[\sum_{i=1}^{n}(q_i - q_{i-1})\log(t - t_{i-1}) + q_n\left\{\log\left(\frac{4k}{\phi\mu c r_w^2}\right) - \gamma\log(e) + 2S\log(e)\right\}\right]$$

where P_w is pressure, P_i is the initial pressure, q_i is the current flowrate, q_{i-1} is the flowrate during the previous step, all under downhole condition. t is current time and t_{i-1} is the time at the last change of the flowrate. The subsequent terms after q_n are for wellbore storage and skin, which are not discussed in this study at least for the time being. m is a coefficient which, in case of re-injection, is given;

$$\frac{kh}{\mu} = \frac{1}{\log e}\frac{1}{4\pi m}$$

where k is permeability, h is thickness of the permeable bed and μ is fluid viscosity.

Obviously the permeability-thickness product kh can be derived once value of m is found. Since downhole pressure has a linear relationship with the term $\Sigma\,(q_i - q_{i-1})\log(t - t_{i-1})$ in the above equation, in ideal condition, plotting these two parameters should yield straight line and its slope as the value of coefficient m. Its result is shown in Fig.10 which seems to show coherent linear relationship between the two parameters, suggesting that the above equation is held valid for this particular example. From the slope, kh was derived as ~0.4 Darcy·m assuming μ as 1.2 x 10^{-4} Pa·sec, which matched remarkably well with the value obtained by the full scale well test.

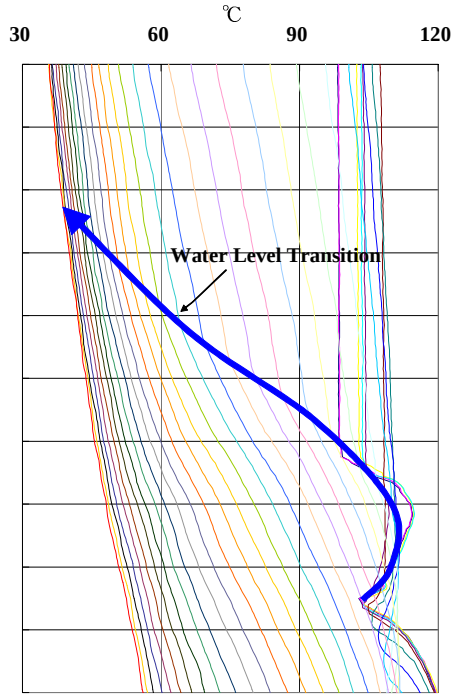

Figure 8. Temperature profiles and water level transition during injecting water.

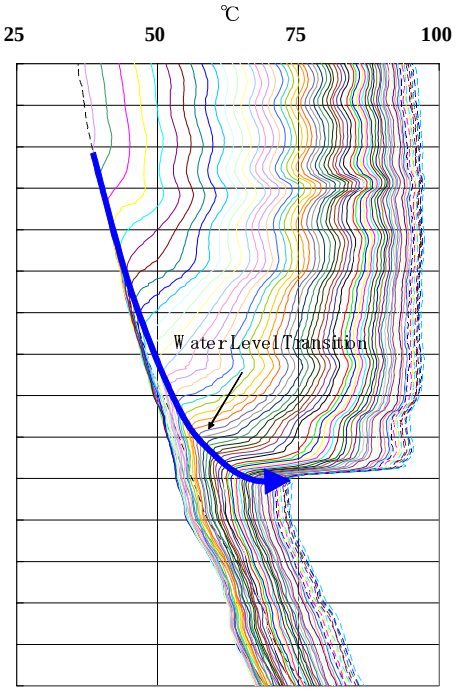

Figure 9. Temperature profiles and water level transition after stopping water injection.

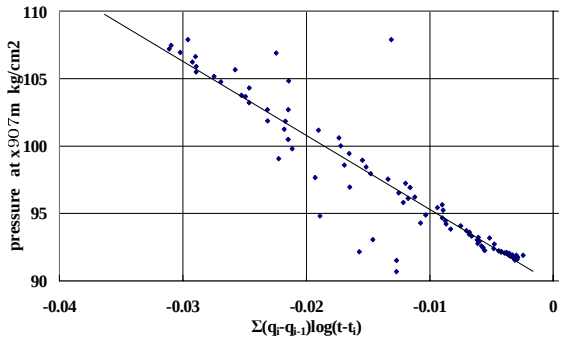

Figure 10. Variable-rate convolution function vs. downhole pressure computed .from fiber-optic temperature data during water injection and subsequent recovery test.

ESTIMATING RESERVOIR PRESSURE

For highly permeable reservoir which almost instantly reaches equilibrium drawdown pressure for given flowrate, Ikeda(2002) demonstrated a way to derive intrinsic reservoir pressure for individual permeable layer from the fiber-optic distributed temperature data. However for wells with poor permeability, that way of interpretation can not be applied as the pressure vs. flowrate has large transient characteristics which can not be dealt by the method referred above.

In this case, what drew our attention was that the transition of the temperature profile during the fall-off. The water level which ascended by more than 200m during water injection, started descending immediately after the injection stopped. Suppose certain difference in intrinsic reservoir pressure for different layers exists, it may occur that while afterflow to one layer is still continuing, one to the other zone may have stopped as it is expected to have lower intrinsic reservoir pressure. The temperature profiles measured after stopping water injection for the well discussed above clearly indicates discontinuity of the flow pattern at the depth where the presence of a permeable bed is expected as shown in Fig.11.

The intrinsic reservoir pressure for individual layers can be derived by the water level and the temperature profile at the time when the flow corresponding to the particular layer is thought ceased. Although this way of analysis does not address the error involved due to transient nature, it yet offer better approximation of the reservoir pressure. In this particular case, the difference of the water head between the layer at around x900 and the one at near bottom is about 80mteres. As for reference, transition of the temperature profiles during water injection is shown in Fig.12 which clearly indicates flowrate changed at the depth as above.

The reservoir pressure for the shallowest layer is deduced by plotting flowrate vs. pressure during water injection and static condition much in the same way as in Ikeda(2002). The reservoir temperature for the second layer was deduced from the temperature profile and the flowrate ratio for the bottom most layer and the second one for the cross flow present under static condition. The interpretation result is shown in Table 1. These reservoir parameters may help to construct a coherent reservoir model which one day enables to predict production output.

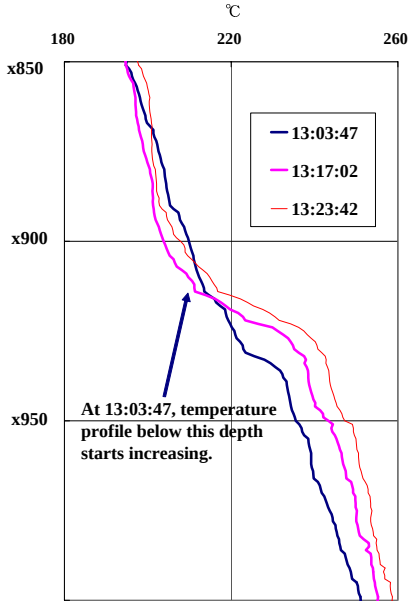

Figure 11. Temperature profiles during post-injection when the water level were descending.

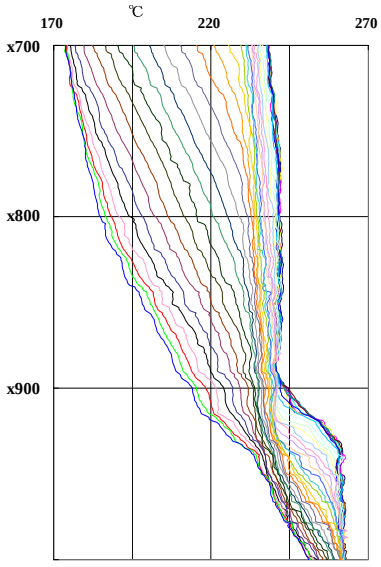

Figure 12. Temperature profiles at around a permeable bed during injecting water.

Permeable zone	Reservoir pressure KSC	Fluid temperature deg. Celsius	*kh* Darcy·m
1	42.15	?	0.15
2	97.24	190	0.14
3	129.17	261	0.11

Table1 Deduced reservoir characteristics.

CONCLUSION

It is demonstrated that the fiber-optic distributed temperature log, when it is properly deployed, literally can visualize the fluid movement occurring in wellbore, which consequently makes it easier to diagnose what is behind causing such phenomena. Since it enables us to access vertically and chronologically undisrupted temperature profiles over the entire wellbore section, hence in a sense undisrupted state of the fluid, it is easier to correlate and/or verify symptoms occurring in different locations along the wellbore, as far as they are in continuous liquid phase.

A method introduced is valid not only for identifying each of highly permeable beds but also for serving quantitative analysis rendering such parameters as intrinsic reservoir pressure, fluid temperature and permeability of each permeable bed. Though the accuracy of the obtained value is yet limited, in large part by the interpretation model utilized, which is often too simple as the transient factors are almost neglected, it should not really be attributed to the limitation of the method itself. The result obtained could serve as essential basis for further studies such as with spinner survey, thus for enhancing interpretation quality.

On the other hand, for the best use of this type of dynamic measurement, the interactive manipulation skill of the operator, backed by good understanding of the tool, the well structure and the reservoir engineering is essential. These include, for example, planning prudent logging procedure for the specific well condition, timely and optimally reacting to the unexpected well response and coordinating with drillers/owner for pumping operation, etc.

ACKNOWLEDGMENT

The study could not be materialized without understanding and support from Kyushu Electric Power Co., Inc. The author would like to express sincere gratitude for it as well as for allowing to use their data.

REFERENCES

Ikeda, N., Uogata, K., Kawazoe, S., Haruguchi, K. (2000). "Delineation on Fracture Type Reservoir by Transient Temperature Monitoring using Fiber Optic Sensor," *Proceedings WGC2000*. C-2-3.

Ikeda, N., (2002), "A novel way to identify fracture and reservoir characteristics by fiber-optic distributed temperature log." *Proceedings, 27th workshop on geothermal reservoir engineering, Stanford University,* SGP-TR-171.

Ikeda, N., (2002) "Fiber-Optic Instantaneous Temperature Profile Log For Geothermal Reservoir Application" *Society of Professional Well Log Analysts, 43rd annual logging symposium transactions* Paper G

Iino, A., Kuwabara, M., Kokura, K. (1990). "Mechanisms of Hydrogen-Induced Losses in Silica-Based Optical Fibers" *Journal of Lightwave Technology,* Vol.8, No.11. pp1675-1679.

Stone, J., (1987). "Interactions of Hydrogen and Deuterium with Silica Optical Fibers: A Review" *Journal of Lightwave Technology,* Vol.LT-5, No.5. pp712-733.

Sumitomo Electeric Industries (1995). "Joint study report on Distributed Temperature Measurement System for Geothermal wells", *Internal Report*

Normann, R., Weiss, J. and Krumhans, J. (2000), "Development of fibers Optic Cables for Permanent Geothermal Wellbore development." *Proceedings, 26th workshop on geothermal reservoir engineering, Stanford University,* SGP-TR-168.

Smithpeter, C., Normann, R., Krumhans, J., Benoit, D. and Thompson, S. (1999). "Evaluation of a distributed fiber-optic temperature sensor for logging wellbore temperature at the Beowawe and Dixie Valley geothermal fields." *Proceedings, 24th workshop on geothermal reservoir engineering, Stanford University,* SGP-TR-162, 329-335.

Stewart, G., et al. (1983). "Afterflow Measurement and Deconvolution in Well Test Analysis." *SPE 58th Annual Technical Conference and Exhibition in San Francisco,* SPE12174.

Simmon J.F., (1986). "Interpretation of Underbalanced Surge Pressure Data by Rate-Time Convolution." *SPE 61st Annual Technical Conference and Exhibition in New Orleans,* SPE15477.

NEDO (1993). "Well Test Manual"

ADDITIONAL NOTE

During the well testing for the well under this study, another intriguing temperature phenomena was seen. In Fig.13, series of temperature profiles are shown

which were taken during water injection above the original water level. It is seen from the original temperature profile that the wellbore had been filled with steam above water level. Once water injection started, it is natural that the temperature starts decreasing from the shallower section and it was the case. However at the same time, at depth where it was expected to be filled with steam, the temperature started rising.

Using this opportunity where various expertise are present, I would like to ask if anybody would be able to provide plausible explanation to the temperature phenomena shown in Fig. 13.

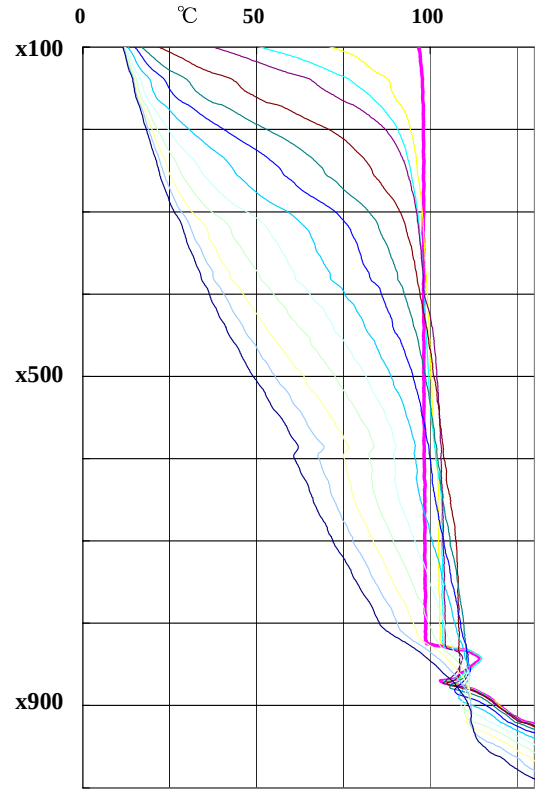

Figure 13. Temperature profiles above water level during injecting water into the well referred through this study.